Available online at www.sciencedirect.com

SciVerse ScienceDirect

Journal of the European Ceramic Society 32 (2012) 2163–2172

www.elsevier.com/locate/jeurceramsoc

# Microstructural comparison of porous oxide ceramics from the system $Al_2O_3$–$ZrO_2$ prepared with starch as a pore-forming agent

Zuzana Živcová-Vlčková[a,b,*], Janis Locs[c], Melanie Keuper[d], Ivona Sedlářová[e], Michaela Chmelíčková[a]

[a] Department of Glass and Ceramics, Institute of Chemical Technology, Prague (ICT Prague), Technická 5, 166 28 Prague 6, Czech Republic
[b] Department of Electrochemical Materials, J. Heyrovsky Institute of Physical Chemistry, v.v.i., Academy of Sciences of the Czech Republic, Dolejškova 3, 182 23 Prague 8, Czech Republic
[c] Riga Technical University, Riga Biomaterials Innovation and Development Center, 3/3 Pulka Street, LV-1007 Riga, Latvia
[d] Institute for Geoscience, Eberhard-Karls-Universität, Wilhelmstrasse 56, D-72074 Tübingen, Germany
[e] Department of Inorganic Technology, Institute of Chemical Technology, Prague (ICT Prague), Technická 5, 166 28 Prague 6, Czech Republic

Received 7 September 2011; received in revised form 31 January 2012; accepted 6 February 2012
Available online 3 March 2012

**Abstract**

In this paper we show examples of microstructures of porous oxide ceramics prepared by traditional slip casting (TSC) and starch consolidation casting (SCC) and present results obtained using different microstructural characterization techniques; Archimedes method (open and total porosity), shrinkage measurement, mercury intrusion porosimetry (pore size distribution) and microscopic methods – optical microscopy with microscopic image analysis (pore size distribution) and scanning electron microscopy (detailed investigation of the local microstructure). In particular, microstructures are compared for porous ceramics from the system $Al_2O_3$–$ZrO_2$ prepared with rice and corn starch. It is shown that maximum values of the total porosity of porous ceramics prepared with starch as a pore-forming agent were approx. 50%. A major finding by using SEM with respect to starch-produced porous ceramics is the existence of pore fillings in the form of small sintered ceramic shell inside the pores, as a result of starch granule shrinkage during the drying and burn-out steps.
© 2012 Elsevier Ltd. All rights reserved.

*Keywords:* Casting; Microstructure – final; Porosity; Electron microscopy; $Al_2O_3$; $ZrO_2$

## 1. Introduction

Ceramic materials are generally, due to their refractoriness and corrosion resistance up to rather high temperatures, widely used especially for high-thermal applications or in chemically aggressive environments. Concerning porous resp. cellular ceramic materials, their major advantage is in the combination of good properties of the ceramic phase with controlled microstructure and with different degrees of porosity. The use of porous ceramic materials is quite diverse today (e.g. thermal and acoustic insulators,[1–5] filters,[6–11] membranes,[12–17] catalyst support,[4,10,18–20] biomaterials,[10,18,21–24] ceramic burners,[10,25,26] gas sensors,[27,28] piezoceramic hydrophones,[29] etc.) and according to the type of application different microstructures and thus different preparation methods are required for porous ceramic bodies. For thermal or acoustic insulators materials with closed porosity are preferred, whereas membranes and filters require open pores with exactly defined pore size. The same can be said about gas burners and about certain bioceramics applications, where important criteria can be open porosity and sufficient pore size (e.g. minimum pore size aperture for tissue ingrowth, especially for bone tissue, is above 100 μm). In the case of catalyst supports a large specific surface area is desired, again in connection with sufficient open porosity and suitable pore size. Very specific

* Corresponding author at: Department of Electrochemical Materials, J. Heyrovsky Institute of Physical Chemistry, v.v.i., Academy of Sciences of the Czech Republic, Dolejškova 3, 182 23 Prague 8, Czech Republic.
Tel.: +420 26605 3446; fax: +420 28658 2307.
*E-mail address:* zuzana.zivcova@jh-inst.cas.cz (Z. Živcová-Vlčková).

0955-2219/$ – see front matter © 2012 Elsevier Ltd. All rights reserved.
doi:10.1016/j.jeurceramsoc.2012.02.005

are the requirements for functional ceramics with controlled porosity, e.g. membranes for solid oxide fuel cells (SOFCs) and piezoelectric PZT ceramics for hydrophones.

One of the preparation methods of porous ceramics is using pore-forming agents (PFAs). Over the last 15 years there has been an increasing interest in PFAs and the development of new preparation methods of porous ceramics, which also leads to use of new principle so-called starch consolidation casting – SCC. This method was designed and for the first time published in the year 1998 by Lyckfeldt and Ferreira.[30] Starch consolidation casting is based on the ability of starch to swell in water at elevated temperature and thus to absorb water from aqueous ceramic suspensions. This behavior enables the preparation of ceramic green bodies by casting starch-containing ceramic suspensions into impermeable molds and heating the system up to approx. 80 °C. When the temperature of the suspension exceeds a certain threshold (i.e. after a certain induction period, dictated by the heating rate of the whole system – suspension and mold), the starch granules begin to swell and, finally, gelatinize. This temperature-induced swelling of the starch granules, followed by subsequent gelatinization, push the ceramic powder particles (which are typically much smaller than the starch granules) together into the interstices between the starch granules and transform the (initially viscous) ceramic suspension into an elastic (i.e. more or less rigid) ceramic body (at this stage called "green body" in ceramic technology), which can subsequently be dried and fired.[31] Benefits of this method (SCC) compared to traditional slip casting (TSC) consist, i.e. in the long durability of molds and the possibility to effectively reduce microstructure gradients. Starch, a natural biopolymer, is suitable for the preparation of porous ceramics especially because the ash content after starch burnout is negligible low.[31] Other important characteristics for selecting PFAs are availability (regarding to the possibility of satisfying long-term demand), low price, environmental aspects and combustion products (from the viewpoint of hygiene and safety). To all these criteria, starch corresponds equally well or better than synthetic pore-forming agents.

In the last few years, concomitantly with the more widespread use of PFAs in ceramic technology, research began to focus on the quantitative comparison of particle size distribution of PFAs and the pore size distribution in the resulting porous ceramics. This comparison is possible only if the microscopic image analysis results, which are primarily number-weighted distributions, are transformed into volume-weighted distributions.[32] Similarly, only after this transformation a comparison of results from microscopic image analysis with mercury porosimetry results is possible. Moreover, the results can be made more precise when an appropriate correction for the random section problem is applied, e.g. the Saltykov transformation.[33] Although the literature is full of works concerned with preparation of porous ceramics using PFAs, including starch, many results of these works are mutually incomparable, because the way of pore size determination is not sufficiently defined and even the concentration measures applied are different. If, e.g. the content of PFA is given in wt.% in the suspension, this quantity has no direct relation to the expected or attainable porosity in the ceramic body, which is defined by the volumetric fraction of pores in the body after burnout (therefore is in this work we have used the so-called nominal content of PFA, i.e. the volume fraction or volume percentage of PFA relative to the ceramic powder).

In this paper we report on the characterization of porous oxide ceramics prepared with starch as a pore-forming agent, in particular the porosity, pore size distribution and SEM investigation of sintered bodies. Porous $ZrO_2$, $Al_2O_3$ and composite $Al_2O_3$–$ZrO_2$ ceramics are prepared by two different shaping methods, traditional slip casting (TSC) and starch consolidation casting (SCC), respectively, and the resulting microstructures are investigated and discussed. As a pore-forming agent starch (rice and corn) is used. In SCC the starch acts at the same time as a body-forming agent.[31,34,35,37]

## 2. Experimental

### 2.1. Materials

Ceramic powders, distilled water, deflocculant, and pore-forming agents were used for sample preparation. Aqueous suspensions have been prepared with commercial alumina powder (α-$Al_2O_3$, *CT 3000 SG*, *Almatis GmbH*, *Germany*; median particle size 0.6 μm, density 4.0 g/cm$^3$), zirconia powder (*t*-$ZrO_2$, *TZ-3YE* stabilized with 5 wt.% $Y_2O_3$, *Tosoh*, *Japan*; median particle size of primary crystallites 26 nm, density 6.1 g/cm$^3$) and $Al_2O_3$–$ZrO_2$ composite powder containing 80 wt.% zirconia and 20 wt.% alumina (ATZ, *ATZ-80*, *Daiichi-Kigenso*, *Japan*; median particle size 0.3 μm, density 5.52 g/cm$^3$), respectively, in the range 65–80 wt.% (content of

Table 1
Composition of alumina ($Al_2O_3$), zirconia ($ZrO_2$) and alumina–zirconia (ATZ) suspension used for traditional slip casting (TSC) and starch consolidation casting (SCC). Values of suspension concentration correspond to several nominal starch contents.

| Preparation method | Type of ceramic | Type of starch | Suspension concentration [wt.%] | Nominal starch content [vol.%] |
|---|---|---|---|---|
| TSC SCC | $Al_2O_3$ | Rice[(only SCC)] | 80 | 10 |
| | | | 78 | 20–25 |
| | | | 75 | 30 |
| | | | 68 | 50 |
| | | Corn | 80 | 10–25 |
| | | | 75 | 30 |
| | | | 70 | 50 |
| | $ZrO_2$, ATZ[(only corn)] | Rice, corn | 70 | 10–35 |
| | | | 65 | 50 |

ceramic powder or ceramic solids loading in the suspension without the additional starch content, Table 1), 1 wt.% (based on alumina), 0.8 wt.% (based on zirconia), 1.5 wt.% (based on alumina–zirconia), respectively, deflocculant (*Dolapix CE 64*, *Zschimmer & Schwarz*, *Germany*) and pore-forming agents (rice starch, *Remy FG*, *Remy Industries NV*, *Belgium*, median particle size 5 μm, density 1.5 g/cm$^3$; corn starch, *Gustin*, *Dr. Oetker a.s.*, *Czech Republic* and *Amioca Powder TF*, *National Starch & Chemical*, *UK*, respectively, median particle size 14 μm, density 1.5 g/cm$^3$) with contents in the range 5–50 vol.% (with respect to the ceramic powder). The suspension concentration (content of ceramic powder) was chosen in order to ensure optimal rheological properties of the suspension required for casting, i.e. with the increasing nominal starch content the content of ceramic powder had to be reduced, which will also include increasing water content in the suspension.

### 2.2. Preparation methods

Two methods were used for the preparation of porous alumina ceramic bodies; traditional slip casting (TSC) into plaster molds (cylindrical rods, diameter 5 mm) and starch consolidation casting (SCC) using metal molds (cylindrical rods, diameter 7 mm). After homogenization for 2 h in polyethylene bottles on laboratory shaker (*HS 26*, *IKA GmbH*, *Germany*) using alumina balls, the suspensions were cast into the molds. The homogeneity of the ceramic suspensions was determined by laser diffraction (presence of agglomerates). Details of the suspension preparation as well as the casting techniques (TSC and SCC) have been previously published in several papers.[31,34,35,37] In the SCC process the filled metal molds were closed (to avoid evaporation) and then were subsequently heated for 2 h at 80 °C to allow the starch to swell. After demolding, the green bodies were dried and subsequently fired (heating rate 2 °C/min, hold time 2 h) at 1570 °C (alumina samples), 1530 °C (composite alumina–zirconia samples) and 1490 °C (zirconia samples), respectively.

### 2.3. Characterization methods

The measurement of integral microstructural descriptors of as-fired porous ceramic (characteristics of densification), i.e. open and total porosity, of the resulting microstructures was performed by the Archimedes method of double-weighing in water. Linear shrinkage was measured using digital slide caliper as an average value from five points on each sample. Pore size distribution was determined by mercury intrusion porosimetry (*AutoPore IV 9500*, *Micromeritcs*, *USA*) and by microscopic image analysis (*Lucia G version 4.81*, *Laboratory Imaging*, *Czech Republic*). For the latter purpose, polished sections were prepared from the as-fired samples and micrographs of the porous microstructures were taken using an optical microscope (*Jenapol*, *Zeiss*, *Germany*). Section area equivalent diameters[36] of the pores were determined by the image analysis software for "manually" selected objects (at least 1500 for each specimen), using area-equivalent circles (fixed by 3-point labeling),[37] and frequency histograms were recorded. Generally the primary microscopic image analysis results are number-weighted size distributions ($q_0$ – distributions/frequency histograms). In order to compare these size distributions with other commonly measured size distributions (e.g. particle size distributions measured by laser diffraction or pore size distributions measured by mercury porosimetry) it is necessary to transform the microscopic image analysis results to volume-weighted distributions ($q_3$ – distributions/frequency histograms). As long as the particle shape is approximately size-invariant, this can be done by the simple formula

$$(q_3)_i = D_i^3 \cdot (q_0)_i, \quad (1)$$

where $(q_0)_i$ is the relative number (frequency) of objects (particles or pores) in the $i$-th size class, $D_i$ is the average size (equivalent circle diameter) of this size class and $(q_3)_i$ is the relative volume of all the objects (particles or pores) in this size class. After performing the $q_0 - q_3$ – transformation the frequency histogram can be summed up ("integrated") in order to obtain a (volume-weighted) cumulative curve ($Q_3$), which can principally be compared with the results of laser diffraction (for particles) and mercury porosimetry (for ceramic microstructures).[32] In the case of pores, however, there is the additional problem, that due to the random 2D section probed in a polished sample the actual pores sizes are principally underestimated (Wicksell's corpuscle problem[38]). The simplest way to manage this problem and to obtain a good estimate for the real 3D pore size distribution from the $Q_3$ – distribution (cumulative) is the so-called Saltykov transformation.[32,33] Microstructural details were investigated on fracture surfaces by scanning electron microscopy – SEM (*Tescan Mira/LMU*, *Czech Republic*), using an accelerating voltage of 15 kV and operating distance of 6–10 mm. Before measurement the samples were coated with a very thin (15 nm) gold layer.

## 3. Results and discussion

### 3.1. Porosity

Figs. 1 and 2 compare the total porosity for all types of porous ceramics prepared with rice and corn starch as a pore-forming agent by TSC and SCC, respectively. From these graphs it can be concluded, that the total porosity of ceramics (after burnout) can be generally controlled by the nominal starch content in the suspension. Total porosity can be readily controlled using TSC, where starch does not undergo any transformation during the forming process (no swelling, no gelatinization). Thus the dependence of total porosity on the nominal starch content displays a relatively steep slope. By contrast, when using the SCC method the slope of this dependence is smaller, i.e. the range of attainable porosities is more restricted and the possibility of porosity control is more limited (on the other hand, from the viewpoint of technological processing, it may be to be an advantage that the porosity is less sensitive to the nominal starch content). The dependence is flatter for rice starch than for corn starch, because rice starch is markedly smaller and undergoes more significant shape changes during swelling and

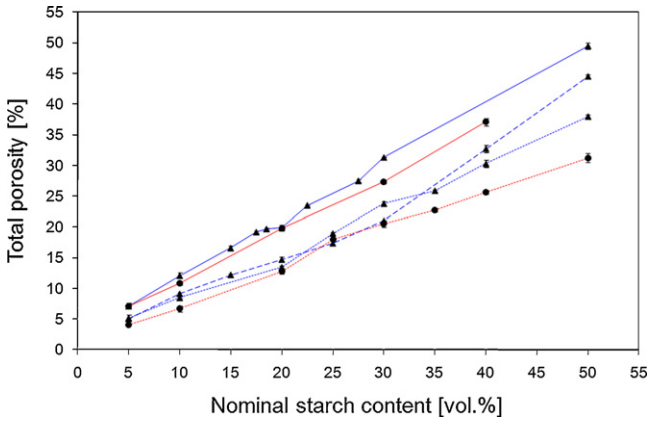


Fig. 1. Total porosity of porous $Al_2O_3$ (full curve), $Al_2O_3$–$ZrO_2$ composite (dashed curve) and $ZrO_2$ (dotted curve) ceramics prepared by traditional slip casting (TSC – full symbols) with rice (circles) and corn (triangles) starch, respectively, as a pore-forming agent.

gelatinization. Further, the different course of the total porosity dependence on the nominal starch content is evident for $Al_2O_3$ (A) and $ZrO_2$ (Z) and $Al_2O_3$–$ZrO_2$ (ATZ) composite ceramics, where $ZrO_2$ is the dominating phase. In all cases the total porosity achieved in ceramics $ZrO_2$ and ATZ ceramics is lower than in $Al_2O_3$ ceramics. This effect is related to the different relative density of green body (after drying) and in principle it was explained by Slamovich and Lange, at least for the case of TSC.[39] It is a well-known empirical fact that $ZrO_2$ powders, when cast from suspensions, form bodies with markedly smaller relative density than $Al_2O_3$ powders, a fact that is closely related to the finding that the solids loading achievable in suspensions suitable for casting is usually much lower for $ZrO_2$ than for $Al_2O_3$. The relative density determined for green bodies prepared by casting suspensions from ceramic powders (without starch or other PFA) are approx. 70–75% for CT-3000 SG powder ($Al_2O_3$) and approx. 49–53% for TZ-3YE powder ($ZrO_2$). It is this relative density that corresponds approximately to the relative density of the matrix between PFA particles, at least in the case of TSC (in the case of SCC this consideration is complicated by the fact, that different swelling may result in different pressures in the matrices between starch particles). Therefore the matrix shrinkage is much larger in the case of $ZrO_2$ ceramics, and thus the total porosity achieved with certain nominal starch content smaller, than in the case of $Al_2O_3$ ceramics.

$Al_2O_3$ and $ZrO_2$ ceramics prepared by SCC with rice starch show an absolutely different course the dependence of total porosity on nominal starch content in the suspension in comparison with $Al_2O_3$, $ZrO_2$ and ATZ ceramics prepared by SCC with corn starch (Fig. 2). It is possible to say, that in the case of oxide ceramics prepared by SCC with rice starch the total porosity is almost independent on the nominal starch content, when the latter is higher than 20–30%. Oxide ceramics prepared by SCC with corn starch with nominal starch contents below approx. 30 vol.% for $ZrO_2$ and ATZ ceramics and below 40 vol.% for $Al_2O_3$ ceramics exhibit higher values of total porosity than the nominal starch content in the ceramic suspension. Above these nominal starch contents (30 resp. 40 vol.%) the total porosity is lower than the nominal starch content.[40,41] This effect may be caused by steric hindrance (excluded volume effect) and/or by an insufficient amount of water available for full swelling of starch granules.

In all cases of oxide ceramics prepared by TSC with rice and corn starch it was found, that below certain values of nominal starch contents the porosity in the ceramic bodies remains essentially closed and above this "critical" value the fraction of open (i.e. apparent) porosity increases more or less abruptly. This effect can be interpreted as percolative in the sense, that from a certain value of total porosity mutual pore contact occurs, and with increasing total porosity a connected pore network is formed throughout the ceramic body. In the case of ceramics prepared by SCC this effect does usually not appear, because the total porosity (due to starch swelling) is usually so high, that the microstructure of body prepared corresponds to a system above the percolation threshold (however, this need not be a common rule, as can be seen from the case of $ZrO_2$ ceramics prepared by SCC with rice starch, see Fig. 3). Fig. 3 shows the dependence of open porosity on total porosity for all those

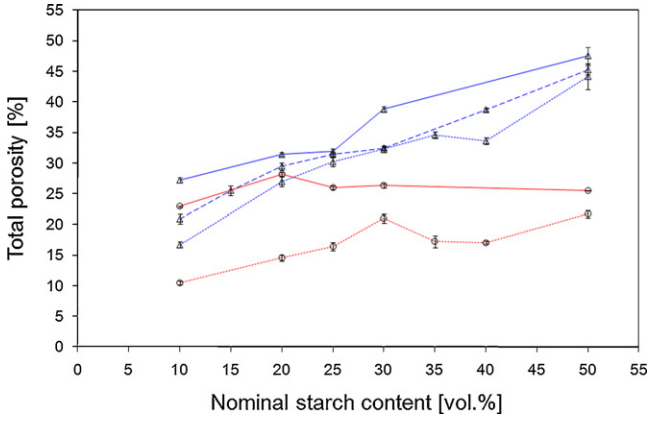


Fig. 2. Total porosity of porous $Al_2O_3$ (full curve), $Al_2O_3$–$ZrO_2$ composite (dashed curve) and $ZrO_2$ (dotted curve) ceramics prepared by starch consolidation casting (SCC – empty symbols) with rice (circles) and corn (triangles) starch, respectively, as a pore-forming agent.

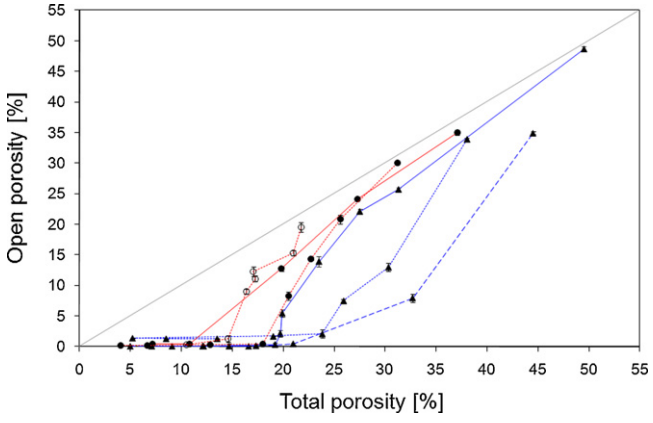


Fig. 3. Percolation threshold of porous $Al_2O_3$ (full curve), $Al_2O_3$–$ZrO_2$ composite (dashed curve) and $ZrO_2$ (dotted curve) ceramics prepared by traditional slip casting (TSC – full symbols) and starch consolidation casting (SCC – empty symbols) with rice (circles) and corn (triangles) starch, respectively, as a pore-forming agent.

systems in the present work for which a percolation of this kind has been observed. Although the values of the percolation threshold from case to case (which is not surprising, because it is known, that the percolation threshold is a very sensitive parameter of the microstructure[42]) it is evident, that most values can be estimated to lie within the range 13–23%, i.e. are approximately $18 \pm 5\%$. This result confirms previous findings on alumina prepared by TSC with corn starch[34] and are is in good agreement with other author's findings.[43]

### 3.2. Shrinkage

Fig. 4 shows a comparison of values of linear shrinkage after burnout as a function of the nominal starch content in the suspension and the ceramic solids loading of the suspensions. It is evident from these diagrams, that in the case of oxide ceramics prepared by TSC, shrinkage is practically independent of the starch content. This finding is in good agreement with the widely acknowledged opinion that the large pores (i.e. pores large in comparison with the particle size of ceramic powder or

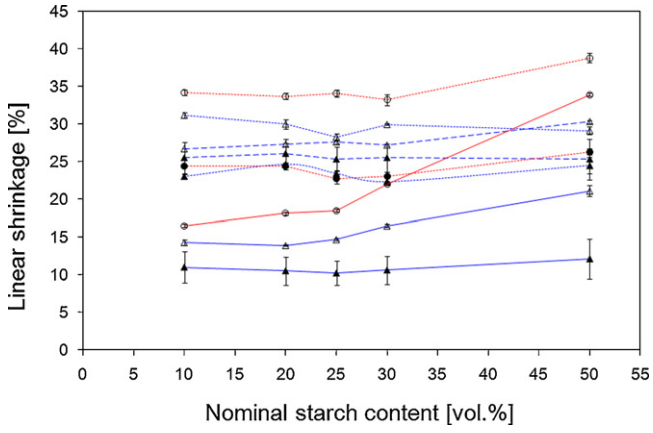


Fig. 4. Linear shrinkage of porous $Al_2O_3$ (full curve), $Al_2O_3$–$ZrO_2$ composite (dashed curve) and $ZrO_2$ (dotted curve) ceramics prepared by traditional slip casting (TSC – full symbols) and starch consolidation casting (SCC–empty symbols) with rice (circles) and corn (triangles) starch, respectively, as a pore-forming agent.

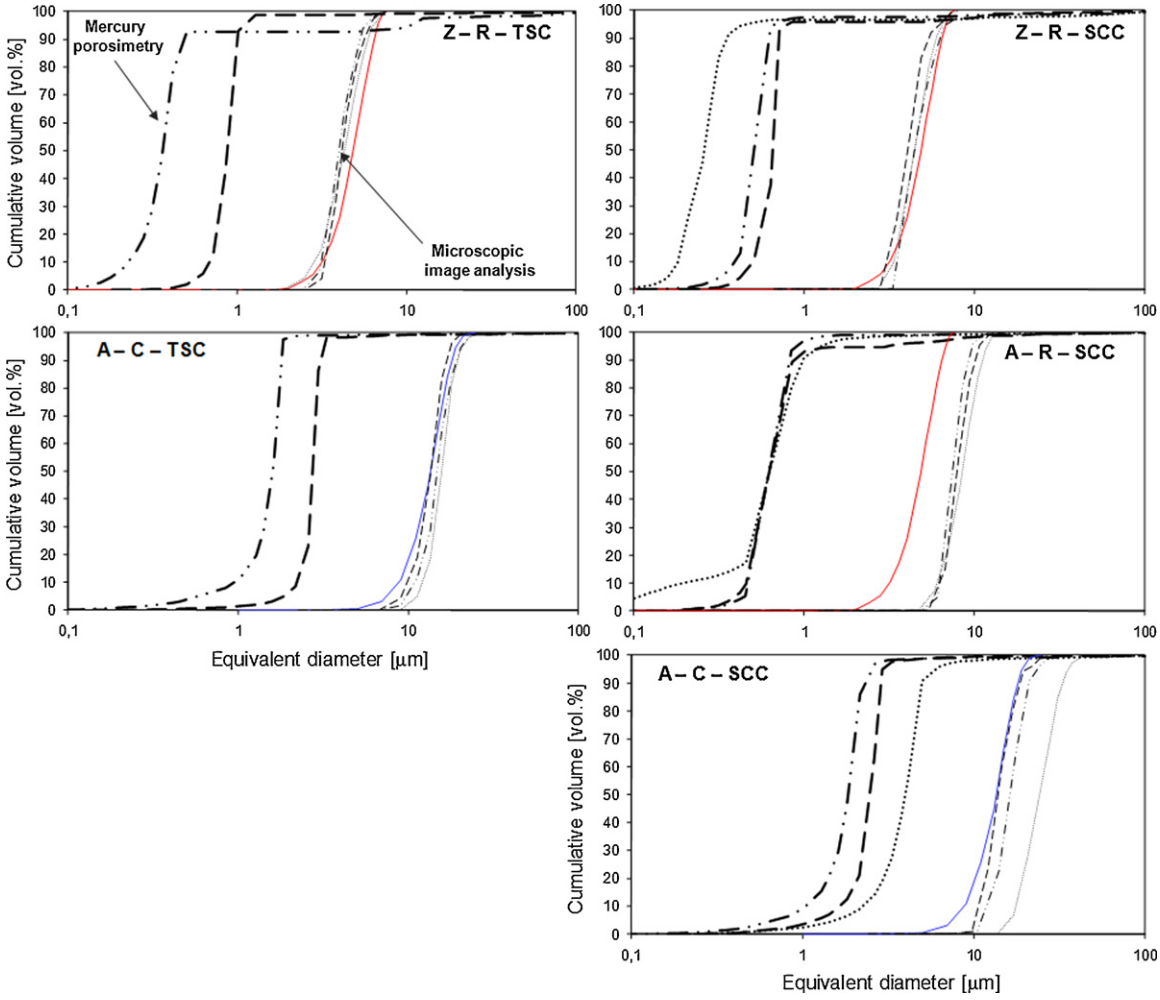


Fig. 5. Volume-weighted ($Q_3$) pore throat size distributions (measured by mercury porosimetry – thick curves on the left side on each diagram) and pore size distributions (measured by microscopic image analysis – thin curves after Saltykov transformation[33] on the right side on each diagram) of porous $Al_2O_3$ (A) and $ZrO_2$ (Z) ceramics prepared by TSC (left) and SCC (right) with nominal starch contents of 10 (dotted curve), 30 (dot-dashed curve) and 50 vol.% (dashed curve); particle size distribution of starch measured by microscopic image analysis, for comparison (full curve).

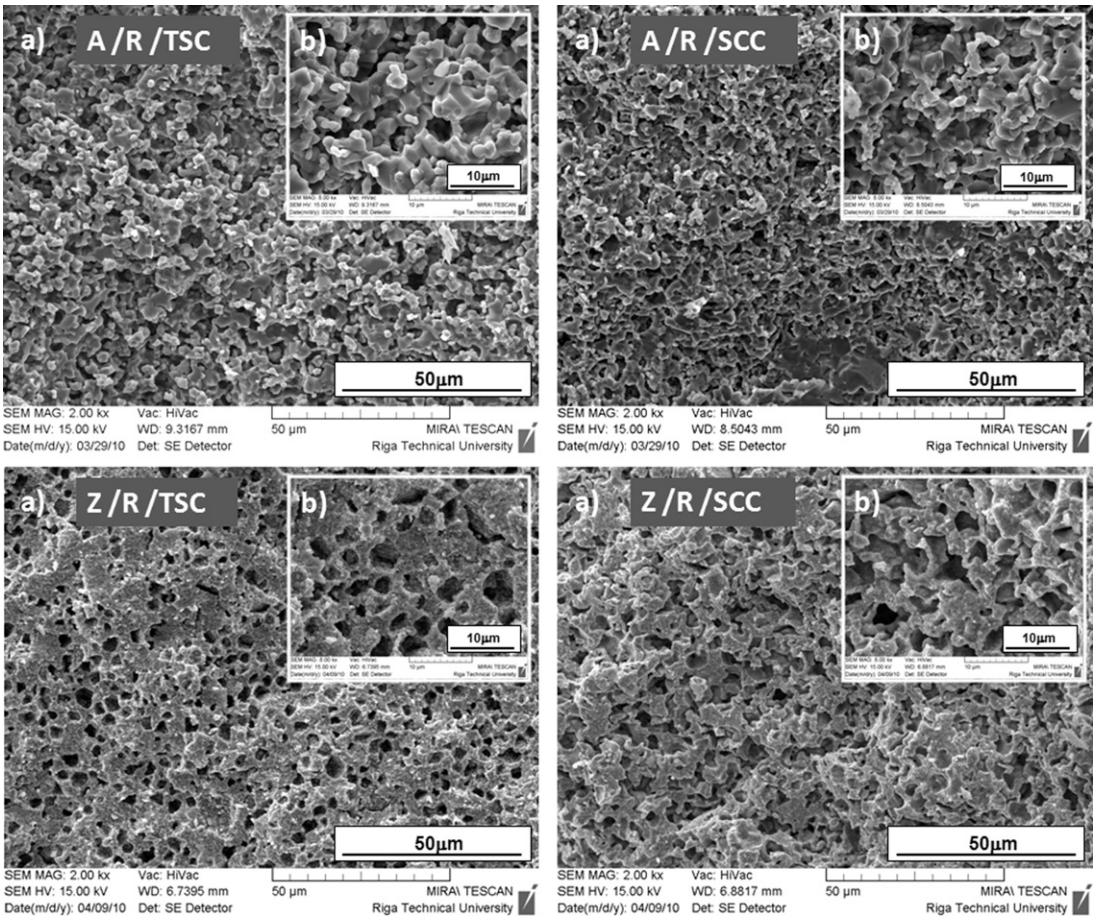


Fig. 6. SEM micrographs (fracture surfaces) of porous $Al_2O_3$ (top) and $ZrO_2$ (bottom) ceramics prepared by traditional slip casting (TSC – left) and starch consolidation casting (SCC – right) with a nominal rice (R) starch content of 30 vol.%; (a) scale bar 50 μm, (b) scale bar 10 μm.

with the grain size constituting the ceramic matrix, or in other words: pores with high coordinating number) do not contribute to the shrinkage of ceramic bodies.[40,44] Linear shrinkage is significantly smaller in $Al_2O_3$ ceramics (approx. 11%) than in $ZrO_2$ ceramics or in ATZ composites (approx. 24–26%). This finding is in good agreement with results from other works, where the linear shrinkage after burnout is for alumina ceramics prepared from identical ceramic powder as in this work (CT 3000 SG) approximately 10–12%[45] and for zirconia ceramics prepared from TZ-3Y powder (similar to powder TZ-3YE, used in this work) approx. 22%.[46] In TSC, where the plaster molds are semipermeable and the packing density of the ceramics particles achieved is determined by the driving force (capillary suction),[34] no dependence of shrinkage has been observed on the ceramic solid loading in the suspension (Table 1). In the case of ceramics prepared by SCC the situation is different. Also in this case shrinkage is smallest for $Al_2O_3$ ceramics, but clearly dependent on starch type (approx. 14% for corn starch and approx. 17% for rice starch with suspension concentration 80 wt.% $Al_2O_3$) and on the ceramic solids loading of the suspension (shrinkage of the ceramic body increases with decreasing suspension concentration). The dependence of shrinkage on the starch type in SCC is due to different swelling kinetics[31] of rice and corn starch and the ensuing different relative density of the ceramic matrix in the green body (different packing density of the ceramics particles after the shaping step). At high starch concentrations could be also higher shrinkage caused by insufficient content of free water in suspension necessary for fully swelling of starch granules leading to reducing the packing density of the ceramics particles between starch particles. For $ZrO_2$ ceramics or ATZ composite ceramics shrinkage is markedly higher (30–34% for $ZrO_2$ and approx. 27% for ATZ) and again dependent on suspension concentration and starch type (in the case of $ZrO_2$ shrinkage is 30% for bodies prepared with corn starch and 34% for bodies prepared with rice starch).

### 3.3. Pore size distribution and SEM micrographs

Results of pore size distribution measurements for $Al_2O_3$ and $ZrO_2$ ceramics are shown in Fig. 5. Generally it is possible to say, that the pore size distributions measured by microscopic image analysis (MIA) have to be interpreted as pore cavity size (diameter) distributions, while the pore size distributions measured by mercury porosimetry (and evaluated via the Washburn equation) correspond to the size distribution of throats or necks connecting two adjacent pores. Hence, median values measured via mercury porosimetry are smaller than median values measured via MIA by approx. one order of magnitude (Tables A1–A3). In

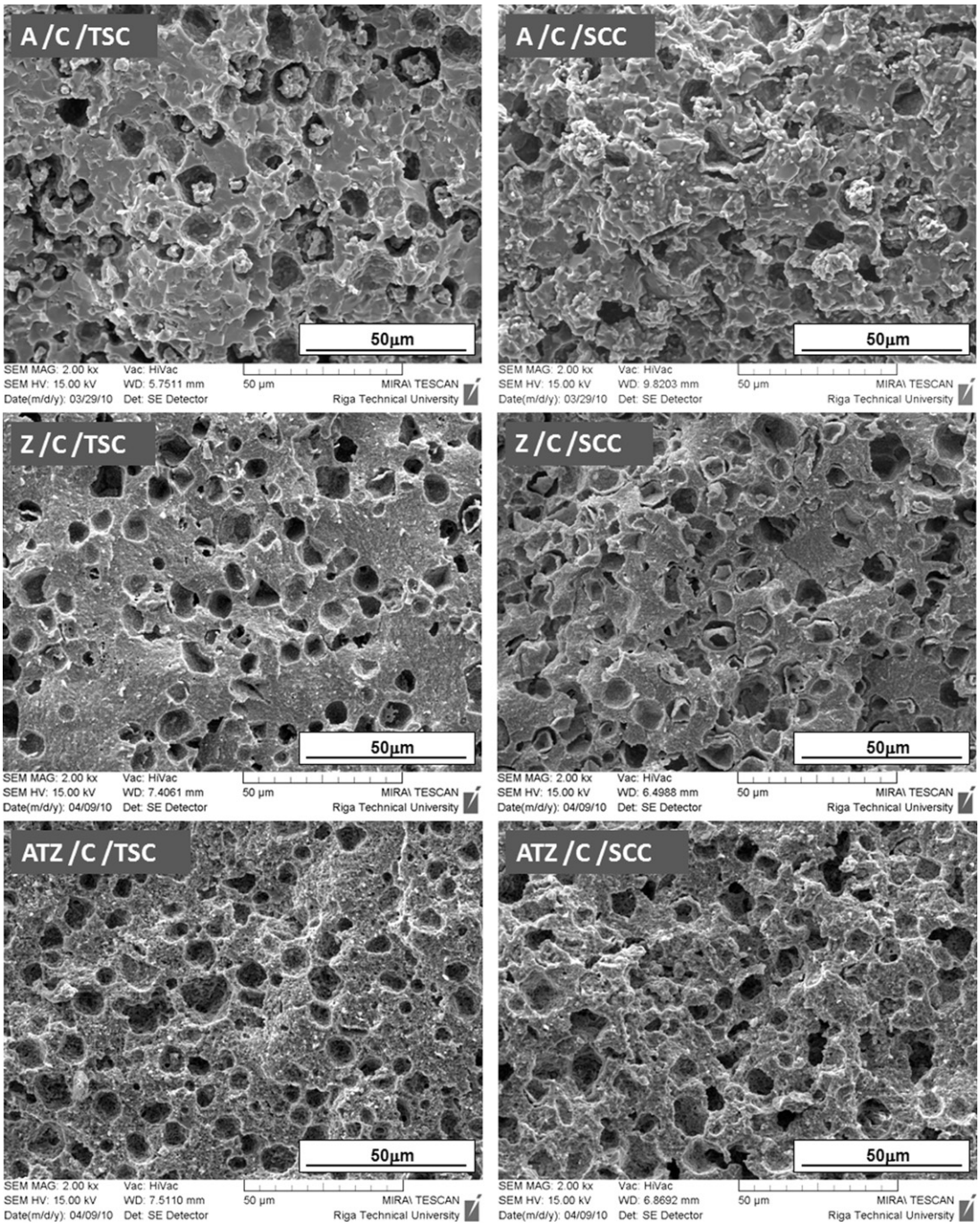


Fig. 7. SEM micrographs (fracture surfaces) of porous $Al_2O_3$ (top), $ZrO_2$ (middle) and $Al_2O_3$–$ZrO_2$ (ATZ) composite ceramics (bottom) prepared by traditional slip casting (TSC – left) and starch consolidation casting (SCC – right) with a nominal corn (C) starch content of 30 vol.%; scale bar 50 µm.

the case of pore size distributions measured by MIA in ceramics prepared by TSC (Fig. 5, left) approximate agreement is evident between these curves and the starch granules size distribution. In ceramics prepared by SCC (Fig. 5, right) the MIA pore size distribution can of course be shifted to larger size than the starch granule size, because of swelling of the starch granules.

Figs. 6 and 7 show microstructures of porous oxide ceramics, prepared by TSC and SCC with rice or corn starch as a pore-forming agent. On some of these SEM micrographs ceramic "shells" are visible inside the pores. In the case of $Al_2O_3$ ceramics prepared by TSC with corn starch (Fig. 7, top left) these shells are clearly visible and most symmetrical. In $ZrO_2$ ceramics the presence of ceramic shells is clearly evident in the case of bodies prepared by SCC (although their character is different from those in $Al_2O_3$), while in the case of ATZ ceramics the pores are empty. Also in the case of ceramics prepared with rice starch the shells inside the pores seem to be absent. The formation of these shells is obviously related to the interaction between particles of ceramic powder and pore-forming agent. However, except for the fact that for pore-forming agents with small particle size (e.g. rice starch) shells were not observed,

see Fig. 6, no general rule as to the appearance or absence of these shells could be ascertained. Nevertheless, the finding in general confirms observations of other authors, who found similar shells in porous ceramics prepared with starch.[41,47,48] In the case of porous ceramics prepared with corn starch, the pore shape is more regular (convex) and the pore size is greater, compared to the case of microstructures prepared with rice starch. However this finding was expected and confirmed the results of our previous work and literature data.

## 4. Conclusions

This paper is devoted to the preparation, characterization and final microstructural comparison of porous oxide ceramics (from the system $Al_2O_3$–$ZrO_2$, i.e. $Al_2O_3$, $ZrO_2$ and ATZ composites) prepared by two different method-traditional slip casting (TSC) and starch consolidation casting (SCC), with starch (rice and corn) as a pyrolyzable pore-forming agent. The porous oxide ceramics were characterized by the Archimedes method (open and total porosity). Maximum values of the total porosity of porous ceramics ($Al_2O_3$, $ZrO_2$ and ATZ composite ceramics) prepared with starch by TSC and SCC was approx. 50%. The total and open (apparent) porosity in the ceramics after firing depends on the amount (nominal content) of starch added to the suspension. Above a total porosity value of approx. $18 \pm 5$% (percolation threshold) the fraction of open porosity increases steeply, and at total porosity values of approx. 50% practically all pores are open. Generally it can be said that the porosity of ceramics can be controlled by the amount (nominal content) of starch added to the suspension and the pore size can be controlled by the type of pore-forming agent. Pore size distributions were measured by microscopic image analysis and mercury porosimetry. In order to compare pore size distributions measured by microscopic image analysis with pore size distributions measured by mercury porosimetry it is necessary to transform the microscopic image analysis results (number-weighted distributions) to volume-weighted distributions. In all cases the neck size between pores (mercury porosimetry) is about one order of magnitude smaller than the size of the pores themselves (microscopic image analysis). Shrinkage after firing is in the case of oxide ceramics prepared by TSC practically independent of the content and type of starch used and also of the concentration (ceramic solids loading) of the suspension. On the other hand, in the case of ceramics prepared by SCC the shrinkage is dependent on the starch type and the concentration of the suspension. SEM micrographs of fracture surfaces showed that a typical feature in some of the microstructures is the presence of a ceramic "shell" inside the pores, which is formed during drying and burnout of the starch. Its presence is, it seems, dependent of the type of starch and ceramic powder, independent of the preparation method (TSC or SCC), and related to the interaction of the ceramic powder with the starch.

## Acknowledgments

This study was part of the project 9008107 "Porous $ZrO_2$ ceramics-preparation and characterization", supported by the ICT Prague. The authors thank E. Gregorová and W. Pabst (ICT Prague).

## Appendix A.

See Tables A1–A3.

Table A1
Pore size (median values) of porous zirconia ($ZrO_2$) ceramics prepared by TSC and SCC with rice starch as a pore forming agent determined by microscopic image analysis and mercury porosimetry.

| $ZrO_2$ ceramic | Median $D_{50}$ [μm] | | | |
|---|---|---|---|---|
| Nominal rice starch content [vol.%] | Microscopic image analysis | | Mercury porosimetry | |
| | Traditional slip casting (TSC) | Starch consolidation casting (SCC) | (TSC) | (SCC) |
| 10 | 4.3 | 4.4 | – | – |
| 25 | – | – | – | 0.26 |
| 30 | 4.0 | 4.5 | 0.36 | 0.50 |
| 50 | 4.2 | 4.0 | 0.87 | 0.65 |

Table A2
Pore size (median values) of porous alumina ($Al_2O_3$) ceramics prepared by TSC and SCC with rice starch as a pore forming agent determined by microscopic image analysis and mercury porosimetry.

| $Al_2O_3$ ceramic | Median $D_{50}$ [μm] | |
|---|---|---|
| Nominal rice starch content [vol.%] | Microscopic image analysis | Mercury porosimetry |
| | Starch consolidation casting (SCC) | |
| 10 | 8.5 | 0.66 |
| 30 | 7.5 | 0.65 |
| 50 | 7.9 | 0.65 |

Table A3
Pore size (median values) of porous alumina ($Al_2O_3$) ceramics prepared by TSC and SCC with corn starch as a pore forming agent determined by microscopic image analysis and mercury porosimetry.

| $Al_2O_3$ ceramic nominal corn starch content [vol.%] | Median $D_{50}$ [μm] Microscopic image analysis | | Mercury porosimetry | |
|---|---|---|---|---|
| | Traditional slip casting (TSC) | Starch consolidation casting (SCC) | (TSC) | (SCC) |
| 10 | 15.7 | 24.0 | – | 4.0 |
| 30 | 14.8 | 16.2 | 1.6 | 1.9 |
| 50 | 13.6 | 13.9 | 2.7 | 2.5 |

## References


1. Scheffler M. *Cellular ceramics*. Weinheim: WILEY-VCH Verlag GmbH & Co. KGaA; 2005.
2. Rice RW. *Porosity of ceramics*. New York: Marcel Dekker, Inc; 1998.
3. Garcia-Ten J, Orts MJ, Saburit A. Thermal conductivity of traditional ceramics Part II: influence of mineralogical composition. *Ceram Int* 2010;**36**:2017–24.
4. Ashby MF. The properties of foams and lattices. *Phil Trans R Soc A: Math Phys Eng Sci* 2006;**364**:15–30.
5. Gregorová E, Živcová Z, Pabst W. Pore-forming agents for the preparation of thermally insulating ceramics. In: Koenig J, editor. *Proceedings of ITCC-29/ITES-17*. 2007. p. 179–89.
6. Colombo P. Conventional and novel processing methods for cellular ceramics. *Phil Trans R Soc A: Math Phys Eng Sci* 2006;**364**:109–24.
7. Zender H, Leistner H, Searle HR. $ZrO_2$ materials for application in the ceramic industry. *Interceram* 1990;**39**:33–6.
8. Gauckler LJ, Waeber MM, Conti C, Jacobduliere M. Ceramic foam for molten-metal filtration. *J Met* 1985;**37**:47–50.
9. Terauchi N, Ohtani T, Yamanaka K, Tsuji T, Sudou T, Ito K. Studies on a biological filter for musty odor removal in drinking water treatment processes. *Water Sci Technol* 1995;**31**:229–35.
10. Jayasinghe SN, Edirisinghe MJ. A Novel method of forming open cell ceramic foam. *J Porous Mater* 2002;**9**:265–73.
11. Wenzel C, Aneziris GC, Tsetsekou A. A Study on application of silicon carbide filters for water purification. In. In: *Proceedings of 10th ECerS conference*. Baden-Baden: Göller Verlag; 2007., ISBN 3-87264-022-4. p. 2073–78.
12. Huang S-Ch, Huang Ch-T, Lu SY, Chou KS. Ceramic/polyaniline composite porous membranes. *J Porous Mater* 1999;**6**:153–9.
13. Suzuki T. A Dense cell culture system for microorganisms using a stirred ceramic membrane reactor incorporating asymmetric porous ceramic filters. *J Ferment Bioeng* 1996;**82**:264–71.
14. Chou K-S, Kao KB, Huang CD, Chen CY. Coating and characterization of titania membrane on porous ceramic supports. *J Porous Mater* 1999;**6**:217–25.
15. Van Gestel T, Kruidhof H, Blank DHA, Bouwmeester HJM. $ZrO_2$ and $TiO_2$ membranes for nanofiltration and pervaporation – Part I. Preparation and characterization of a corrosion-resistant $ZrO_2$ nanofiltration membrane with a MWCO < 300. *J Membr Sci* 2006;**284**:128–36.
16. Shqau K, Mottern ML, Yu D, Verweijw H. Preparation and properties of porous α-$Al_2O_3$ membrane supports. *J Am Ceram Soc* 2006;**89**:1790–4.
17. Hu XJ, Chen WD, Huang Y. Fabrication of Pd/ceramic membranes for hydrogen separation based on low-cost macroporous ceramics with pencil coating. *Int J Hydrogen Energy* 2010;**35**:7803–8.
18. Hirschfeld DA, Li TK. Processing of porous oxide ceramics. *Key Eng Mater* 1996;**115**:65–79.
19. Roumanie M, Delattre C, Mittler F, Marchand G, Meille V, Bellefon C, et al. Enhancing surface activity in silicon microreactors: use of black silicon and alumina as catalyst supports for chemical and biological applications. *Chem Eng J* 2008;**115**:S317–26.
20. Vernoux P, Guth M, Li X. Ionically conducting ceramics as alternative catalyst supports. *Electrochem Solid-State Lett* 2009;**12**:E9–11.
21. Kelly BA. Why engineer porous materials? *Phil Trans R Soc A* 2005;**364**:5–14.
22. Rambo CR, Cao J, Seiber H. Preparation of highly porous biomorphic YSZ ceramics. *Mater Chem Phys* 2004;**87**:345–52.
23. Jones AC, Arns CH, Hutmacher DW, Milthorpe BK, Sheppard AP, Knackstedt MA. The correlation of pore morphology, interconnectivity and physical properties of 3D ceramic scaffolds with bone ingrowth. *Biomaterials* 2009;**30**:1440–51.
24. Laasri S, Taha M, Laghzizil A, Hlil EK, Chevalier J. The effect of densification and dehydroxylation on the mechanical properties of stoichiometric hydroxyapatite bioceramics. *Mater Res Bull* 2010;**45**:1433–7.
25. Fuse T, Kobayashi N, Hasatani M. Combustion characteristics of ethanol in a porous ceramic burner and ignition improved by enhancement of liquid-fuel intrusion in the pore with ultrasonic irradiation. *Exp Therm Fluid Sci* 2005;**29**:467–76.
26. Garcia E, Osendi MI, Miranzo P. Thermal diffusivity of porous cordierite ceramic burners. *J Appl Phys* 2002;**92**:2346–9.
27. Coi YJ, Seeley Z, Bandyopadhyay A, Bose S, Akbar SA. Aluminum-doped $TiO_2$ nano-powders for gas sensors. *Sens Actuators B* 2007;**124**:111–7.
28. Akbar S, Dutta P, Lee Ch. High-temperature ceramic gas sensors: a review. *Int J Appl Ceram Technol* 2006;**3**:302–11.
29. Palmqvist L, Lindqvist K, Shaw C. Porous multilayer PZT materials made by aqueous tape casting. *Key Eng Mater* 2007;**333**:215–8.
30. Lyckfeldt O, Ferreira JMF. Processing of porous ceramics by 'starch consolidation'. *J Eur Ceram Soc* 1998;**18**:131–40.
31. Živcová Z, Gregorová E, Pabst W. Low- and high-temperature processes and mechanisms in the preparation of porous ceramics via starch consolidation casting. *Starch/Stärke* 2010;**62**:3–10.
32. Gregorová E, Živcová Z, Pabst W, Sedlářová I. Characterization of porous ceramics by image analysis and mercury porosimetry. *Ceramika-Ceramics* 2006;**97**:219–30.
33. Saltykov SA. *Stereology*. New York: Springer Verlag; 1967.
34. Gregorová E, Živcová Z, Pabst W. Porosity and pore space characteristics of starch-processed porous ceramics. *J Mater Sci* 2006;**41**:6119–22.
35. Gregorová E, Živcová Z, Pabst W, Černý M, Kolomazník P. Porous alumina–zirconia composite ceramics prepared by starch consolidation casting. In: Bućko MM, Haberko K, Pedzich Z, editors. *Proceedings of the 11th international conference and exhibition of the european ceramic society (ECERS-11)*. Cracow: Polish Ceramic Society; 2009., ISBN 978-83-60958-54-4. p. 564–68.
36. Russ JC, DeHoff RT. *Practical stereology*. 2nd ed. New York: Kluwer Academic/Plenum Publishers; 2000.
37. Gregorová E, Živcová Z, Pabst W. Starch as a pore-forming and body-forming agent in ceramic technology. *Starch/Stärke* 2009;**61**:495–502.
38. Wicksell SD. The corpuscle problem – second memoir: case of ellipsoidal corpuscles. *Biometrika* 1926;**18**:151–72.
39. Slamovich EB, Lange FF. Densification of large pores: I. Experiments. *J Am Ceram Soc* 1992;**75**:2498–508.
40. Garrido LB, Albano MP, Plucknett KP, Genova L. Effect of starch filler content and sintering temperature on the processing of porous 3Y-$ZrO_2$ ceramics. *J Mater Process Technol* 2009;**209**:590–8.
41. Barea R, Osendi MI, Miranzo P. Fabrication of highly porous mullite materials. *J Am Ceram Soc* 2005;**88**:777–9.
42. Sahimi M. *Applications of percolation theory*. London: Taylor & Francis; 1994.

43. Albano MP, Garrido LB, Plucknet K. Influence of starch content and sintering temperature on the microstructure of porous yttria-stabilized zirconia tapes. *J Mater Sci* 2009;**44**:2581–9.
44. Diaz A, Hampshire S. Characterisation of porous silicon nitride materials produced with starch. *J Eur Ceram Soc* 2004;**24**:413–9.
45. Chmelíčková M. Alumina ceramics with porosity gradients. Bachelor thesis. Prague: ICT Prague; 2008 (in Czech).
46. Chmelíčková M. Preparation and characterization of oxide ceramics with porous microstructure. Master thesis. Prague: ICT Prague; 2010 (in Czech).
47. Mattern A, Huchler B, Staudenecker D, Oberacker R, Nagel A, Hoffmann MJ. Preparation of interpenetrating ceramic–metal composites. *J Eur Ceram Soc* 2004;**24**:3399–408.
48. Garcia-Gabaldon M, Perez-Herranz V, Sánchez E, Mestre S. Effect of porosity on the effective electrical conductivity of different ceramic membranes used as separators in electrochemical reactors. *J Membr Sci* 2006;**280**:536–44.